

Analysis, Design and Demonstration of a Dual-Reflectarray Antenna in Ku-band for European Coverage

Carolina Tienda¹, Jose A. Encinar², Mariano Barba², and Manuel Arrebola³

¹Department of Radar Concepts, Microwave and Radar Institute, DLR
Oberpfaffenhofen, 82234, Germany
Carolina.Tienda@dlr.de

²Department of Electromagnetism and Circuit Theory Universidad Politécnica de Madrid, ETSIT
Ciudad Universitaria s/n, Madrid, E-28040, Spain
encinar@etc.upm.es, mbarba@etc.upm.es

³Department of Electrical Engineering (Group of Signal Theory and Communications)
Universidad de Oviedo, Gijón (Asturias), E-33203, Spain
arrebola@tsc.uniovi.es

Abstract — An accurate technique has been proposed for the analysis of dual-reflectarray antennas, which takes into account the angle of incidence of the field impinging on main reflectarray cells. The technique has been applied to the analysis and design of a contoured beam antenna in Ku-band that provides a European coverage. The reflected field on the sub-reflectarray is computed using Spectral-Domain Method of Moments assuming local periodicity, as customary. The sub-reflectarray is divided in groups of elements and the radiation from each group is used to compute the incident and reflected fields on the main reflectarray cells. Different degrees of accuracy can be achieved depending on the number of groups considered. A 50-cm antenna demonstrator has been manufactured and measured in a compact range. The measured radiation patterns are in good concordance with the simulations and practically fulfill the coverage requirements with a cross-polar discrimination better than 25 dB in the frequency band 12.975 GHz - 14.25 GHz.

Index Terms — Antenna, countered beam, dual-reflectarray.

I. INTRODUCTION

Reflectarray antennas present a competitive performance for applications like long distance communications [1], spaceborne antennas for contoured beams [2,3] and Synthetic Aperture Radar (SAR) [4], when compared with phased arrays and reflector antennas. Reflectarrays are manufactured by photo-etching and bonding processes which are a well-established technology in multi-layer printed circuit boards (PCB). The reduced bandwidth of the printed

elements used on the reflectarrays and the differential spatial phase delay limit the total bandwidth in reflectarrays [5,6]. To overcome this problem, different techniques have been applied, such as the use of several layers of patches [7,8], multi-resonant elements [9], aperture-coupled patches with delay lines [10], or faceted configurations [11].

Although, single reflectarray antennas have been deeply studied in the last years, dual reflector configurations present some advantages with respect to single reflectarrays [12,13]. Two of these advantages are the reduction of the volume of the antenna for a large focal distance and the possibility of using a small reflectarray subreflector with a main large parabolic reflector. The last configuration combines the broadband and high gain capabilities of parabolic reflectors with the advantage of using a small reflectarray that can be used to improve the behavior of the antenna. In this kind of antennas, the sub-reflectarray can be used to correct the errors in the surface of the very large deployable reflectarrays [14] or to provide beam scanning in a limited angular range [13,15]. The beam can be reconfigured or scanned when the phase-shift on the reflectarray subreflector is electronically controlled by using MEMS [16-18], pin diodes [19], varactor diodes [20,21], or liquid crystals (LC) [22-24] for frequencies around 100 GHz and beyond.

The main, the sub-or both reflectors in a dual-reflector configuration can be replaced by reflectarrays [14,15,25]. Antennas implemented with two reflectarrays [25] as shown in Fig. 1 (a), one as sub-reflector and the other as main-reflector, provide phase control in both surfaces which gives additional degrees of freedom that can be used to improve the performance of the antenna

for certain applications. The bifocal antenna principle applied to dual reflectarray antennas can be used for designing multi-beam antennas providing a stable performance for all beams as shown in [26]. Dual reflectarray antennas implemented with two flat reflectarrays have a high degree of compactness. In dual reflectarray antennas, the beam can be scanned or reconfigured by controlling the phases at the elements of the sub-reflectarray while using the main reflectarray for additional functionalities or improvements in the antenna performance. The sub reflectarray can be also used to change the linear polarization of the feed horn to circular. Applications of this kind of antenna configuration can be Synthetic Aperture Radar (SAR) [27] and radiometric remote-sensing [15].

The accurate analysis of a dual-reflectarray antenna is difficult and requires a high computational effort, since for every single element of the main reflectarray all the field contributions radiated by the cells of the sub-reflectarray must be considered. An analysis technique has been recently reported for the analysis of dual-reflectarray antennas [25], in which the reflection coefficients on the elements of both reflectarrays are computed by Spectral-Domain Method of Moments (SD-MoM) [28] assuming local periodicity. A reflection matrix, which relates the incident and reflected fields, should be computed for every pair of cells in the main and sub-reflectarray. Since the computation of the reflection coefficients $NMR \times NSR$ times was computationally unaffordable, being NMR and NSR the number of cells in the main and sub-reflectarrays respectively, the impinging electric field on every cell of the main reflectarray was approximated by a single plane wave. In this approximation, the incident plane wave is computed as the superposition of the fields coming from every sub-reflectarray cell. The field reflected on every cell of the main reflectarray was computed approximating the incidence angle by that coming from the center of the sub-reflectarray (fix angle of incidence). The approximation reduces significantly the computation time, since each reflection coefficient matrix is computed NMR , instead of $NMR \times NSR$ times. When the phase response of the cells in the main reflectarray is practically no affected by the incidence angles from different sub-reflectarray cells, this approximated approach will provide an accurate analysis on the main reflectarray. In many practical configurations, incidence angles up to 30 degree produce a negligible effect on the response of the main reflectarray cells. The approximate technique was successfully used in [29] to design a compact dual-reflectarray antenna in Ku-band that produces a pencil beam with gain better than 32 dBi and a cross-polar discrimination (XPD) better than 30 dB in a 20% bandwidth (12.2 GHz - 15 GHz), covering Tx and Rx frequency bands. To ensure the validity of the

approximation, the reflectarray elements on the main reflectarray were chosen to be almost insensitive to the angle of incidence. They were made of a single layer of varying-sized patches in a small period ($0.4\lambda \times 0.4\lambda$ at 15 GHz, which is the highest frequency). The experimental results showed a good concordance with the simulations, even though the incidence angles on the main reflectarray were up to 50° in some extreme elements.

The approximation of the fix angle of incidence used in the main reflectarray may not be accurate in many cases, when other reflectarray elements more sensitive to the angle of incidence are used, or when large angles of incidence exist in the antenna configuration. Furthermore, when the antenna is used to produce a contoured beam as in Direct Broadcast Satellite (DBS) applications [2,3,30], the phase errors produce a more drastic distortion in the contoured radiation patterns than in the simple case of a pencil beam, as demonstrated in [3].

The high performance in broadband and cross-polarization achieved by dual-reflectarray configurations shown in [29] for a pencil beam can be also extended to contoured beams for Tx-Rx DBS antennas with high requirements in coverage and cross-polarization [31]. Up to the knowledge of the authors, the only dual-reflectarray prototype designed to produce a shaped beam (sectored in azimuth) was reported in [33], for the particular case of a centered configuration with the reflectarray subreflector placed on a polarizing grid, which limits the operation to single polarization.

In this paper, an analysis technique is presented to provide an accurate and flexible model for dual-reflectarray antennas, which improves the simulation accuracy by taking into account the angles of incidence in each element of the main reflectarray. A dual-reflectarray antenna demonstrator has been completely designed and analyzed using the proposed technique to produce a contoured beam for DBS European coverage. To simplify manufacturing, a limited size demonstrator of 50 cm is implemented, although a larger aperture of approximately one meter should be necessary for a real coverage. The antenna optics has been chosen to limit the total phase variation on the two reflectarrays to a range of 360° to eliminate any need for phase-delay elements. The idea that motivated this paper is to demonstrate that the coverage can be achieved in both transmit and receive frequency bands by using a dual-reflectarray configuration that emulates a large F/D ($F/D=4$). An appropriate analysis technique for dual reflectarray configurations has been applied and validated in the present paper to produce a contoured beam. The antenna was manufactured and measured at Universidad Politécnica de Madrid and the results show good performance in coverage and cross-polarization in the entire working band (12.975-14.250 GHz).

II. GENERAL ANALYSIS TECHNIQUE FOR DUAL-REFLECTARRAY ANTENNAS

The proposed dual-reflectarray configuration comprises a feed-horn and two flat reflectarrays with the phasing elements arranged in a rectangular lattice. The analysis method described here can be used for a flat sub-reflectarray (SRA) and a flat main reflectarray (MRA) with any type of reflectarray elements, including single or multiple layers of patches. The analysis technique consists of four main steps as explained in [25]. The sub-reflectarray is analyzed as a single reflectarray through SD-MoM considering local periodicity. For the analysis of the main reflectarray cells, the sub-reflectarray is divided in groups of elements, and the field radiated by each group with its incident angle is used to compute the reflection response on every main reflectarray cell by SD-MoM. Finally, the radiation pattern is computed from the field on the main reflectarray by applying FFT. This is a very general analysis technique since it provides the chance of making the analysis with different degrees of accuracy and efficiency, by dividing the sub-reflectarray in higher or lower number of groups. The demanded analysis accuracy will depend on the antenna geometry, which defines the maximum angles of incidence on the main reflectarray, on the period and type of cells used in the main reflectarray. $\mathbf{R}_{(p,q)}(m,n)$ matrix represents the reflection coefficients of every cell of the main reflectarray (m,n) for a plane wave coming from each cell of the sub-reflectarray (p,q), this matrix depends on the positions of the cells (m,n) and (p,q) in the main and sub-reflectarrays, and therefore on the angle of incidence. Note that, if the $\mathbf{R}_{(p,q)}(m,n)$ matrix is computed for all combinations of cells (m,n) – (p,q) an extremely long CPU time will be required.

In a dual-reflectarray antenna when the reflectarray subreflector is small and far from the main reflectarray, every field contribution coming from the different cells of the sub-reflectarray are very similar. Thus, there is practically no difference in the computation of the reflection coefficient if the origin of the incident field is considered to be the center of the sub-reflectarray, in this case the effect of the angle of incidence can be neglected ($\mathbf{R}_{(p,q)}(m,n) \approx \mathbf{R}(m,n)$) as in [25]. However, if the main reflectarray cells are located in the near field zone of the sub-reflectarray, the incidence angle can vary strongly for some sub-reflectarray cells. This effect can be neglected if the two sub-reflectarray cells are neighbors but it is strong if they are far away one from each other. To consider this effect, the sub-reflectarray is divided in groups of elements. The incident field on every element of the main reflectarray is decomposed in waves radiated by each group. Each group of cells of the sub-reflectarray produces an electric field contribution in every single cell of the

main reflectarray. Each of these contributions has a different incidence angle, which is taken into account in the computation of the reflected coefficients for each cell in the main reflector. Therefore, for every cell of the main reflectarray, a number of NG reflected coefficients are calculated, being NG the number of groups. The size of the groups is calculated such that the main reflectarray cells fulfill the far field conditions with respect to each group in the sub-reflectarray. For simplicity the size of the groups is maintained constant, although near the reflectarray edge the groups may have some elements left, particularly when the reflectarray subreflector is not rectangular, see Fig. 1 (b).

The field contributions of the cells integrating a group are added before computing the corresponding $\mathbf{R}(m,n)$ matrix on the main reflectarray. All these field contributions are considered to leave from the center of their group. The incident and reflected field on every (m,n) cell of the main reflectarray due to one group of cells is shown in Eq. (1) and Eq. (2) respectively:

$$\mathbf{E}_{\text{inc}(g)}^{X/Y}(m,n) = \sum_{r=1}^{\text{Size}_x} \sum_{s=1}^{\text{Size}_y} \mathbf{E}_{\text{inc}(r,s)}^{X/Y}(m,n), \quad (1)$$

Size_x and Size_y are the number of elements for each group “g” in the x- and y-axis respectively. $\mathbf{E}_{\text{inc}(g)}^{X/Y}(m,n)$ is the electric field impinging on the cell (m,n) of the main reflectarray from the group of cells (g) of the sub-reflectarray, according to Fig. 1 (b), for X or Y polarization. The field reflected at each cell (m,n) of the MRA is:

$$\mathbf{E}_{\text{ref}}^{X/Y}(m,n) = \sum_{g=1}^{NG} \mathbf{R}_{(g)}(m,n) \cdot \mathbf{E}_{\text{inc}(g)}^{X/Y}(m,n), \quad (2)$$

where

$$\mathbf{R}_{(g)}(m,n) = \begin{pmatrix} \rho_{(g) \text{ } xx}^{(m,n)} & \rho_{(g) \text{ } yx}^{(m,n)} \\ \rho_{(g) \text{ } xy}^{(m,n)} & \rho_{(g) \text{ } yy}^{(m,n)} \end{pmatrix}, \quad (3)$$

$\mathbf{R}_{(g)}(m,n)$ is the reflection matrix for the cell (m,n) of the main reflectarray due to the group g. The components $\rho_{(g) \text{ } xx}^{(m,n)}$ and $\rho_{(g) \text{ } yx}^{(m,n)}$ are the direct and cross polarization reflection coefficients for an incident wave polarized with the electric field on X_{SR} direction (without component in Y_{SR}). On the other hand, $\rho_{(g) \text{ } yy}^{(m,n)}$ and $\rho_{(g) \text{ } xy}^{(m,n)}$ are the reflection coefficients for an incident electric field on Y_{SR} direction.

For this general analysis method, there are two possible limit cases: the full-wave case, in which each group of sub-reflectarray elements has only one cell, and the case based on the approximation of fix angle of incidence, in which there is only one group of elements in the sub-reflectarray. In the first case, the electric field coming from each cell of the sub-reflector impinges on each cell of the main reflectarray with different angle, which is taken into account in the computation of the

field reflected by each cell in the main reflectarray. In the opposite case, a unique angle of incidence is assumed for all the field contributions arriving from sub-reflectarray elements, as described in [25].

Finally, the co-polar and cross-polar radiations patterns are computed from the field on the main reflectarray by applying an Inverse Discrete Transform.

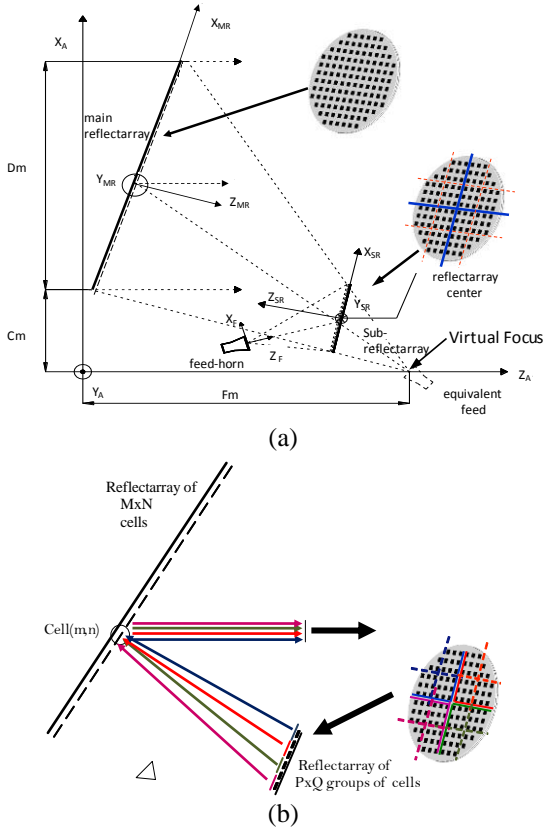


Fig. 1. Scheme of a dual reflectarray structure (a). Scheme of a dual reflectarray structure with the sub-reflectarray divided in groups of elements (b).

III. DESIGN OF A CONTOURED BEAM DUAL-REFLECTARRAY ANTENNA

A dual-reflectarray demonstrator of limited size is designed to provide a European coverage. The antenna optics parameters are given in Table 1 and they are similar to the dual-offset configuration presented previously in [29], considering the same feed-horn, sub-reflectarray, and relative positions respect to the main reflectarray. The phase-shift distribution on the SRA is defined to emulate a hyperbolic subreflector in order to provide an equivalent parabolic system with a large F/D ($F/D=4$), which reduces the range of phase-shift required in the subreflector to eliminate the steps of 360° . However, in this work the phase-shift distribution on the MRA is synthesized to produce a contoured beam that provides European coverage.

Table 1: Geometrical parameters of the dual-reflectarray antenna

Main Reflectarray (MRA)	
Main reflectarray dimensions	41 × 37 elements
Rows x columns	492 mm × 444 mm
Period	12 mm × 12 mm
Sub-Reflectarray (SRA)	
(Data in main reflectarray coordinate system)	
Center coordinates	(-217, 0, 370) mm
Direction cosines matrix (Relates MRA and SRA coordinate systems)	$\begin{bmatrix} 0.715 & 0 & 0.698 \\ 0 & -1 & 0 \\ 0.698 & 0 & -0.715 \end{bmatrix}$
Sub-reflectarray dimensions	380 mm × 380 mm
Rows x columns	38 × 38 elements
Period	10 mm × 10 mm
Feed-Horn	
(Data in sub-reflectarray coordinate system)	
Coordinates of phase-center	(193.73, 0, 635.54) mm
Intersection of feed axis and SRA	(15, 0, 0) mm

The sub-reflectarray is illuminated by a corrugated horn operating in dual-linear polarization, vertical (V) and horizontal (H), with the electric field polarized towards the Y_F and X_F axes, respectively. The antenna position on the satellite is assumed with the Y_{MR} axis perpendicular to the Equator and pointing the North, so that V-polarized field is parallel to Y_{MR} . Since the same coverage is considered for both linear polarizations, the antenna can operate in dual circular polarization by simply using a dual-circular feed. For this antenna configuration the reflectarray subreflector is placed on the Fresnel-zone of the corrugated horn, and therefore a near-field model of the feed-horn [35,36] should be used for an accurate analysis. The incident field on the sub-reflectarray is computed from the field radiated by the feed represented by a spherical wave expansion [37]. The feed-horn produces an illumination taper of -13.48 dB at the sub-reflectarray edges and -16.24 dB at the main reflectarray edges.

The phase shift required on the sub-reflectarray surface is calculated through ray tracing. The phase-shift at each cell is proportional to the difference of the distances from the cell to the feed and to the virtual focus as shown in [29], see Fig. 1 (a).

A. Phase synthesis for European coverage

The European coverage to be synthesized is referred to a geostationary satellite located at $10^\circ E$ longitude and 0° latitude. For the limited sized demonstrator, a minimum gain of 25 dBi is required in the enlarged European region defined in [32], which accounts for the satellite pointing errors. This enlarged coverage is plotted in solid blue line in Fig. 2. The main reflectarray is designed with a phase distribution

synthesized to produce a contoured beam that provides this coverage. Note that a simple coverage has been chosen because of the limited size of the main reflectarray (45 cm x 50 cm). More stringent requirements as shown in [31], or higher levels of gain can be achieved using a more realistic size of the main reflectarray, at least 1 meter for Ku-band antennas.

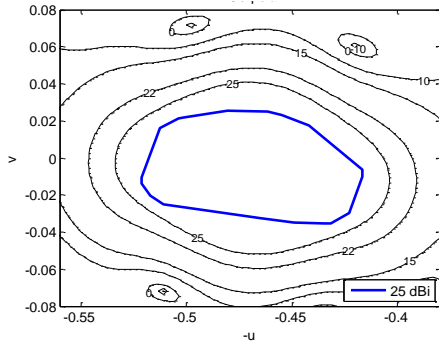


Fig. 2. Synthesized radiation pattern for vertical polarization at 13.75 GHz superimposed to the coverage mask.

A phase-only synthesis technique based on the intersection approach [38] is used to obtain the phase distribution on the main reflectarray surface to produce the required contoured beam. The intersection approach [38] has been successfully used in the design of contoured-beam reflectarrays for DBS antennas [30,31]. The phase-shift to be implemented on the reflectarray is obtained as the difference between the phase of the field obtained from the pattern synthesis and the phase corresponding to the distance from the virtual focus to each cell of the main reflectarray, since the sub-reflectarray is emulating a field radiated by the virtual focus. Considering this phase distribution, the calculated radiation pattern is superimposed to the required mask for the European coverage in Fig. 2. The radiation pattern fulfills the coverage requirements but the gain contours are not able to accurately match the coverage contour because of the limited size of the antenna demonstrator.

B. Design of main and sub-reflectarrays

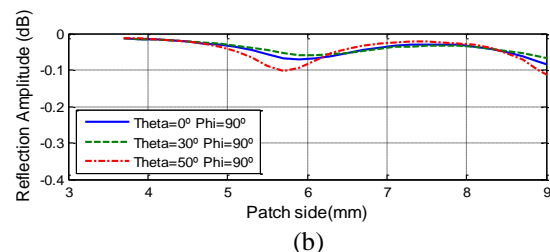
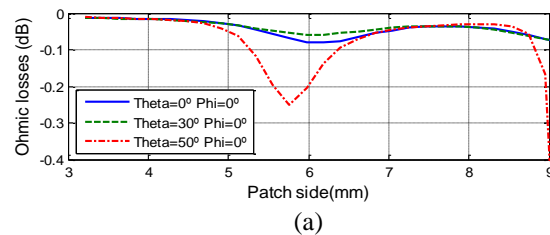
Once the illumination and the phase distribution are determined, the design is carried out for both reflectarrays, considering dual-linear polarizations at 13.75 GHz. The patch dimensions are obtained by the iterative process described in [7] that calls an analysis routine based on SD-MoM [28] assuming local periodicity. The sub-reflectarray has been designed as described in [29]. The same sandwich configuration is used for both the main and sub reflectarrays. The sandwich stack-up, including the thickness and electrical properties of each layer are provided in Table 2. In the two-layer

main reflectarray, the patches are distributed in a rectangular lattice within an ellipse of 492 mm x 444 mm. The selected period is 12 mm in x- and y-axes, thus the main reflectarray is arranged in 41 x 37 elements. The period of the elements in the sub reflectarray is 10 mm in x- and y-axis and they are arranged in a grid of 38 x 38 elements.

Table 2: Lay-up of the sandwich and radio-electric characteristics of the materials

Dielectric/Metallization	ϵ_r	$\tan \delta$	Thickness (mm)
Copper (printed patch layer 2)	-	-	0.05
(SRA) Cuclad 217LX/ (MRA) Diclad 880B	2.17	0.0009	1.524
(SRA/MRA) Cuclad 6250 (thermoplastic bonding film)	2.32	0.0013	0.038
Copper (printed patch layer 1)	-	-	0.05
(SRA) Cuclad 217LX/ (MRA) Diclad 880B	2.17	0.0009	1.524
Copper (ground plane)	-	-	0.05

For both reflectarrays, the phase-shift as a function of the patch size for the design frequency (13.75 GHz) present a practically linear variation covering a phase range of around 400° when the patch size on the first layer vary from 4-mm to 9-mm, for incidence angles up to 50° as can be seen in Figs. 3 (c and d) for both linear polarizations. The losses in the reflectarray cells are very low, with an average value less than 0.1 dB, see Figs. 3 (a and b). For an incidence of 50°, the phase can vary up to 80° in the main and 30° in the sub-reflectarray, respect to normal incidence. For the angle of incidence $\theta=50^\circ$ and $\phi=0^\circ$ in the main reflectarray, the losses drastically increases when the patch length is 9 mm due to a resonance. Note that the elements with an incident angle of 50° are near the edge with an illumination 10 dB below than in the center and their effect is less significant in the radiation pattern.



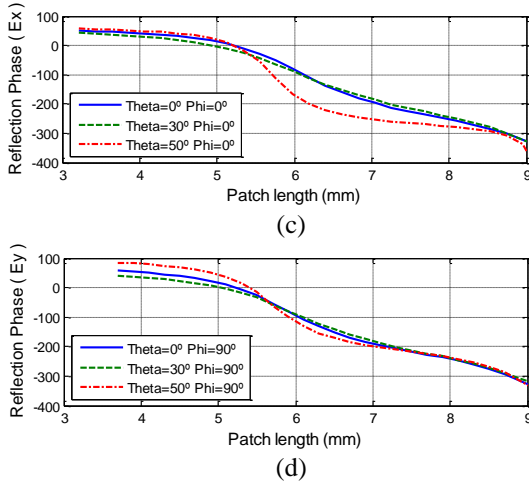


Fig. 3. Reflection coefficient vs. the patch length in the first layer for the cell used in the main reflectarray for (a) amplitude and (c) phase of E_x field component at $\varphi = 0^\circ$ (horizontal polarization), and (b) amplitude and (d) phase of E_y field component, $\varphi = 90^\circ$ (vertical polarization) at 13.75 GHz.

IV. SIMULATIONS AND EXPERIMENTAL RESULTS

The previously designed dual-reflectarray antenna has been analyzed by the technique described in section II under different degrees of accuracy. First, a full wave analysis is considered, when the elements in the sub-reflectarray are considered individually, without grouping ($\text{Size}_x=1, \text{Size}_y=1$). As a second case, the main reflectarray is analyzed using the approximation of the fix incidence angle. Then, the division of the sub-reflectarray aperture is used to analyze the antenna, when dividing the sub-reflectarray in a high number of groups, the radiation pattern are getting closer to those obtained with the full wave analysis:

The number of groups in the sub reflectarray to fulfill the far field conditions with every cell of the main reflectarray is computed, considering the minimum distance between the sub and the main reflectarrays, 23.6 cm. The diameter of one group in the sub should be at least 5 cm to fulfill far-field conditions and between 5 cm and 14 cm to be in the Fresnel zone. If the period in the sub reflectarray is 10 mm, every group of elements has at least 5 elements in each direction, groups of 5×5 elements will fulfill the far field and groups with more than 5×5 elements and less than 14×14 elements will be in Fresnel zone. Taking into account that the sub reflectarray has 38×38 elements, when grouping 13×13 elements, 9 groups are considered in the analysis and when grouping 8×8 elements, 25 groups are considered in the analysis. In both cases, the elements of the main reflectarray closer to the sub reflectarray are in the Fresnel Zone, nevertheless most of the elements in the

main reflectarray with 25 groups in the sub reflectarray fulfil the far field conditions.

The contoured co-polar patterns for the full wave approach (black line) are superimposed in Fig. 4 with those obtained when the sub-reflectarray is divided in 1 (red line), 9 (blue line) and 25 (green line) groups, for both linear polarizations. As expected, the green line converges to the black one. Also when the reflectarray is divided in 3×3 groups (blue line) a good agreement is observed in the main beam. Note that for V-polarization the agreement in the main beam is reasonable under the assumption of fix angle of incidence (one group), because the sensitivity with the angle of incidence of the reflectarray elements is lower for patch dimensions smaller than 9 mm, as shown in Fig 3.

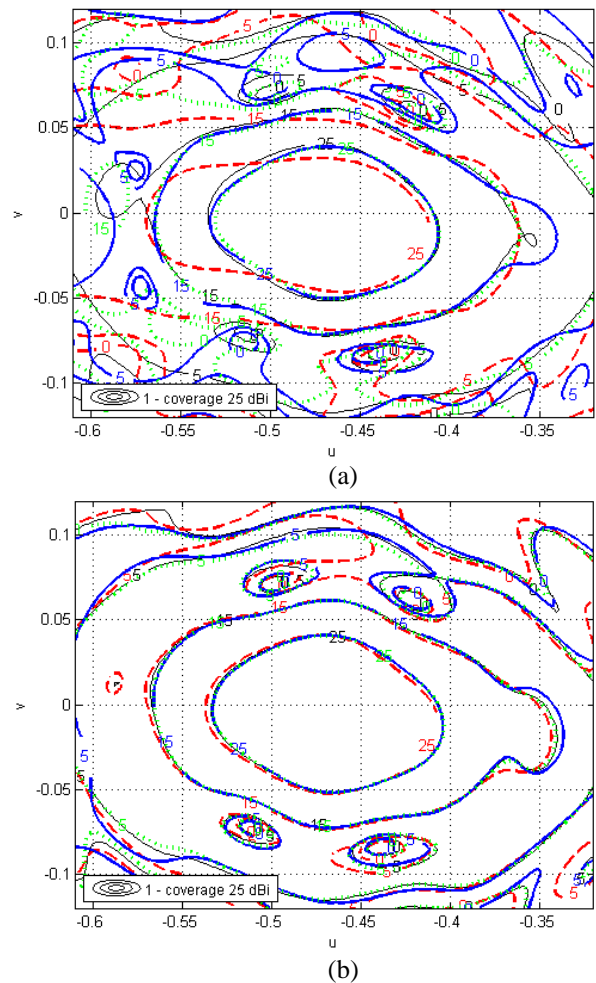


Fig. 4. Contour plots of the copolar components of the radiation pattern for vertical polarization (a) and horizontal polarization (b) simulated for the full wave analysis (solid black line (-)), approximate case (dashed red line (--)) and the more general approach dividing the sub-reflectarray in 9 (dashed dot blue line(-.-)) and in 25 (dashed green line(:)) groups.

Figure 5 shows the antenna demonstrator in the Compact Test Range of Universidad Politécnica de Madrid. The antenna has been measured at the center and at the edges of the frequency band (12.975 GHz, 13.75 GHz and 14.25 GHz). The measured radiation pattern practically fulfils the mask to provide the European coverage with more than 25 dBi gain at the three measured frequencies. The measured and simulated (considering 25 groups) co-polar radiation patterns are superimposed for both linear polarizations at 13.75 GHz in Figs. 6 (a)-(b). A good agreement is observed between simulated and measured patterns, although there are small discrepancies as consequence of a small misalignment between the two layers of printed patches on the main reflectarray. The mentioned misalignment produces phase errors of up to 30° in certain areas of the reflectarray, where the angles of incidence are higher. These errors have been considered in the simulations and compared again with measurements in Figs. 6 (c)-(d), showing a better agreement. The behavior of the antenna is very stable in the required frequency band (12.975 GHz - 14.250 GHz) as shown in Fig. 7. Figure 8 shows the levels of the cross-polarization measured for both linear polarizations at 13.75 GHz. The level of the cross-polar discrimination in the entire frequency band is greater than 25 dB.

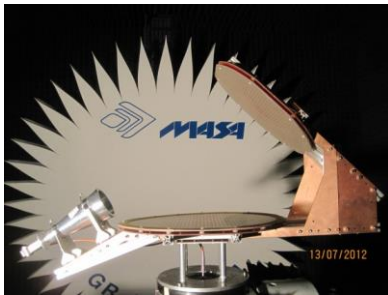


Fig. 5. Dual reflectarray antenna for contoured beam in the compact range anechoic chamber.

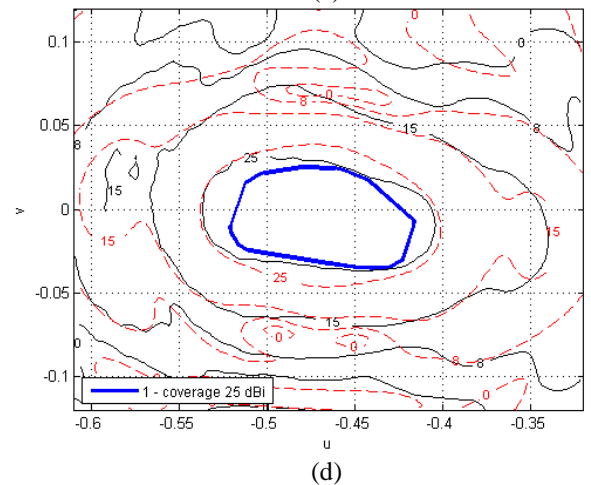
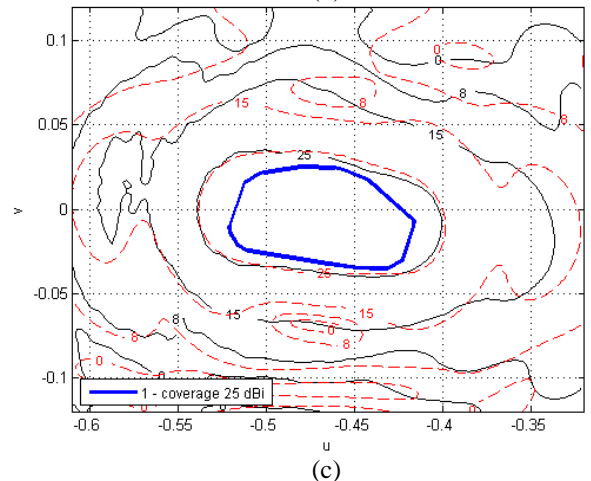
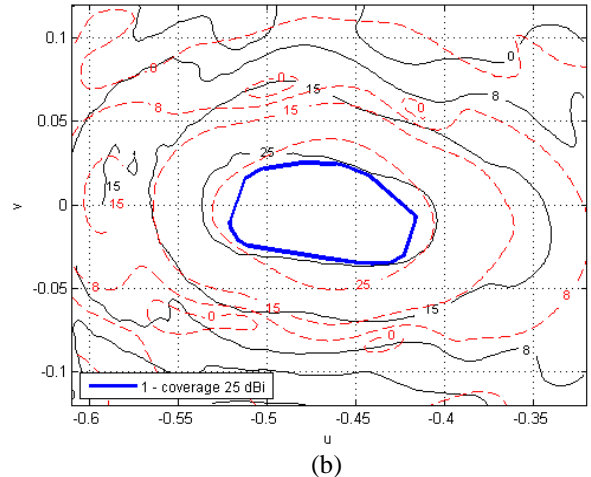
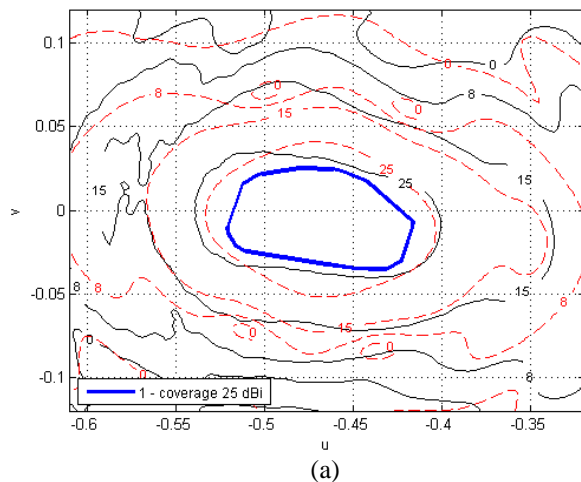
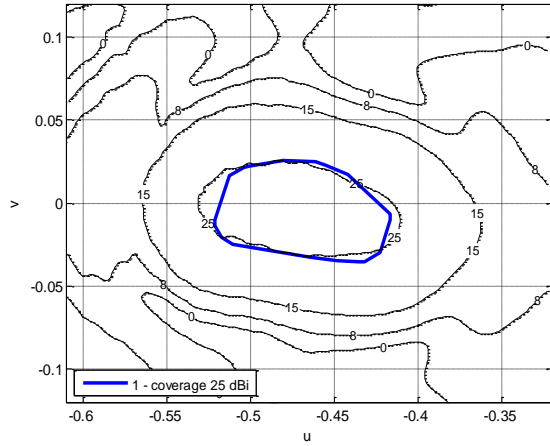
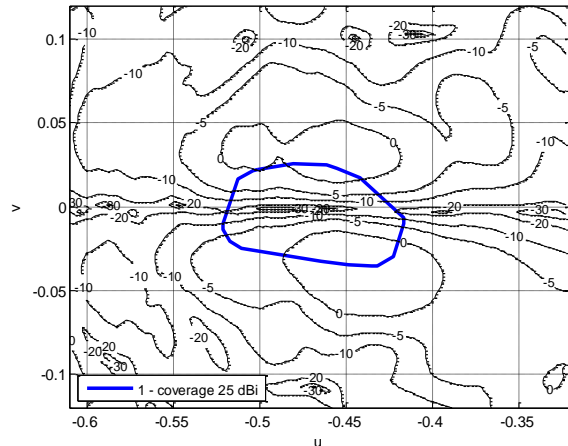


Fig. 6. Contour plots of the simulated copolar components of the radiation pattern (dashed red line (---)), measurements (solid black line (-)) and the mask (thicker solid blue line) for vertical (a) and horizontal (b) polarizations at 13.75 GHz. The simulations are repeated accounting for the phase errors (red line) and compared with measurements for vertical (c) and horizontal (d) polarizations.

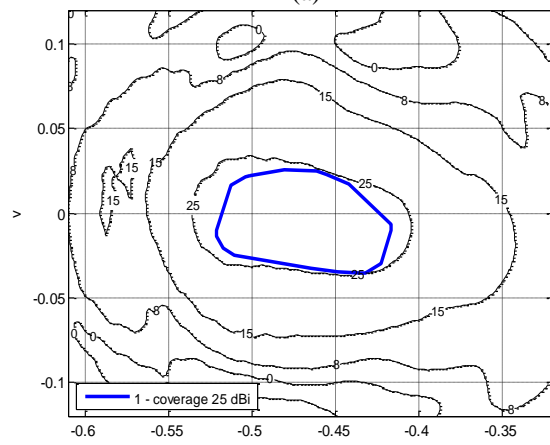


(a)



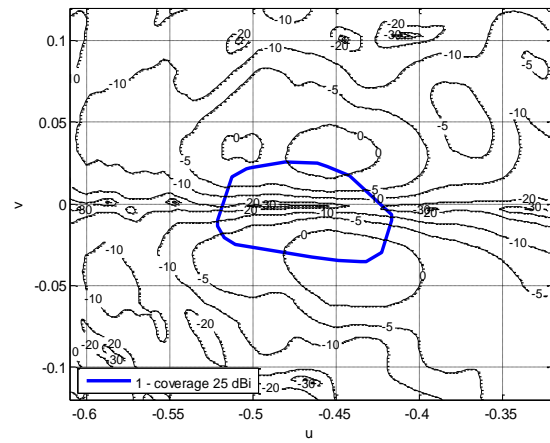
(b)

Fig. 8. Measured contoured plots of the cross-polar components of the radiation pattern (solid black line) superimposed to the coverage mask (thicker solid blue line) for vertical (a) and horizontal (b) polarizations at 13.75 GHz.



(b)

Fig. 7. Measured contoured patterns in dBi (solid black line) superimposed to the coverage mask (thicker solid blue line) for vertical polarizations at 12.975 GHz (a) and 14.25 GHz (b).



(a)

V. CONCLUSION

An accurate analysis technique has been proposed and demonstrated for dual-reflectarray antennas. In the analysis, the sub-reflectarray is divided in groups of elements and the radiation of each group is used to compute the incident and reflected field on each cell of the main reflectarray. The number of groups can be increased to improve the accuracy at the cost of higher computation time. The method of analysis has been validated by designing, manufacturing and testing a limited-size antenna demonstrator with a main reflectarray of 45 cm x 50 cm that provides a contoured beam in dual linear polarization for a DBS European coverage. The measured radiation patterns show a good concordance with the simulations. However, some slight differences in the shape of the beam are observed as consequence of the tolerance errors in the manufacturing process. The antenna provides a cross-polar discrimination higher than 25 dB and a stable performance in the working frequency bandwidth, from 12.975 GHz to 14.25 GHz.

The results obtained with the limited-sized antenna demonstrator shows the capability of the proposed dual-reflectarray configuration to design contoured beam space borne antennas in Ku-band with low levels of cross-polarization. This dual-reflectarray configuration can also be used for multi-spot antennas in Ka-band, since the capability of adjusting the phase distribution simultaneously in both surfaces can be used to design multifocal antennas.

REFERENCES

- [1] J. Huang and J. A. Encinar, *Reflectarray Antennas*. IEEE Press, John Wiley, 2008.
- [2] D. M. Pozar, S. D. Targonski, and R. Pokuls, "A shaped-beam microstrip patch reflectarray," *IEEE Trans. Antennas Propagat.*, vol. 47, no. 7, pp. 1167-1173, 1999.
- [3] J. A. Encinar and J. A. Zornoza, "Three-layer printed reflectarrays for contoured beam space applications," *IEEE Trans. Antennas Propagat.*, vol. 52, no. 5, pp. 1138-1148, 2004.
- [4] H. Legay, B. Salome, E. Girard, S. Ramongassie, J. A. Encinar, and G. Toso, "Reflectarrays antennas for SAR missions," *Proc. Int. Symp. on Antenna Technology and Applied Electromagnetics*, Saint-Malo, France, June 2005.
- [5] J. Huang, "Bandwidth study of microstrip reflectarray and a novel phased reflectarray concept," *IEEE Antennas and Propagation Society Intl. Symp.*, pp. 582-585, June 1995.
- [6] D. M. Pozar, "Bandwidth of reflectarrays," *Electr. Lett.*, vol. 39, no. 21, pp. 1490-1491, 2003.
- [7] J. A. Encinar, "Design of two-layer printed reflectarrays using patches of variable size," *IEEE Trans. Antennas Propagat.*, vol. 49, no. 10, pp. 1403-1410, 2001.
- [8] J. A. Encinar and J. A. Zornoza, "Broadband design of three-layer printed reflectarrays," *IEEE Trans. Antennas Propagat.*, vol. 51, no. 7, pp. 1662-1664, 2003.
- [9] M. R. Chaharmir, J. Shaker, M. Cuhaci, and A. Ittipiboon, "A broadband reflectarray antenna with double square rings," *Microw. Opt. Technol. Lett.*, vol. 48, no. 7, pp. 1317-1320, 2006.
- [10] E. Carrasco, J. A. Encinar, and M. Barba, "Bandwidth improvement in large reflectarrays by using true-time delay," *IEEE Trans. Antennas Propagat.*, vol. 56, no. 8, pp. 2496-2503, 2008.
- [11] H. Legay, D. Bresciani, E. Labiole, R. Chiniard, E. Girard, G. Caille, D. Calas, R. Gillard, and R. Toso, "A 1.3 m faceted reflectarray in Ku band," *15th International Symposium on Antenna Technology and Applied Electromagnetics (ANTEM)*, pp. 1-4, June 2012.
- [12] B. Khayatian, Y. Rahmat-Samii, and J. Huang, "Radiation characteristics of reflectarray antennas: methodology and applications to dual configurations," *Proceeding of First European Conference on Antennas and Propagation*, Nice, France, Nov. 2006.
- [13] M. Arrebola, L. Haro, and J. A. Encinar, "Analysis of dual-reflector antennas," *IEEE Antennas and Propagation Magazine*, vol. 50, no. 6, pp. 39-51, 2008.
- [14] S. Xu, Y. Rahmat-Sami, and W. A. Imbriale, "Subreflectarrays for reflector surface distortion compensation," *IEEE Trans. Antennas Propagat.*, vol. 57, no. 2, pp. 364-372, 2009.
- [15] H. Wenfei, M. Arrebola, R. Cahill, J. A. Encinar, V. Fusco, H. S. Gamble, H. Y. Alvarez, and F. Las-Heras, "94 GHz dual-reflector antenna with reflectarray sub-reflector," *IEEE Trans. Antennas Propagat.*, vol. 57, no. 10, pp. 3043-3050, 2009.
- [16] R. Sorrentino, "MEMS-based reconfigurable reflectarrays," *The Second European Conference on Antennas and Propagation*, Edinburgh, UK, Nov. 2007.
- [17] J. Perruisseau-Carrier and A. K. Skriverviky, "Monolithic MEMS-based reflectarray cell digitally reconfigurable over a 360-phase range," *IEEE Antennas and Wireless Propagation Letters*, vol. 7, pp. 138-141, 2008.
- [18] E. Carrasco, M. Barba, B. Reig, C. Dieppedale, and J. A. Encinar, "Characterization of a reflectarray gathered element with electronic control using ohmic RF MEMS and patches aperture-coupled to a delay line," *IEEE Trans. Antennas Propagat.*, vol. 60, no. 9, pp. 4190-4201, 2012.
- [19] E. Carrasco, M. Barba, and J. A. Encinar, "X-Band reflectarray antenna with switching-beam using PIN diodes and gathered elements," *IEEE Trans. Antennas Propagat.*, vol. 60, no. 12, pp. 5700-5708, 2012.
- [20] M. Riel and J. J. Laurin, "Design of an electronically beam scanning reflectarray using aperture-coupled elements," *IEEE Trans. Antennas Propagat.*, vol. 55, no. 5, pp. 1260-1266, 2007.
- [21] S. V. Hum, M. Okoniewski, and R. J. Davies, "Realizing an electronically tunable reflectarray using varactor diode-tuned elements," *IEEE Microwave and Wireless Components Letters*, vol. 15, no. 6, pp. 422-424, 2005.
- [22] A. Mössinger, R. Marin, S. Mueller, J. Freese, and R. Jakoby, "Electronically reconfigurable reflectarrays with nematic liquid crystals," *IEEE Electronics Letters*, vol. 42, pp. 899-900, 2006.
- [23] W. Hu, R. Cahill, J. A. Encinar, R. Dickie, H. Gamble, V. Fusco, and N. Grant, "Design and measurement of reconfigurable millimeter wave reflectarray cells with nematic liquid crystal," *IEEE Trans. Antennas Propagat.*, vol. 56, no. 10, pp. 3112-3117, 2008.
- [24] G. Perez-Palomino, P. Baine, R. Dickie, M. Bain, J. A. Encinar, R. Cahill, M. Barba, and G. Toso, "Design and experimental validation of liquid crystal-based reconfigurable reflectarray elements with improved bandwidth in F-Band," *IEEE Trans. Antennas Propagat.*, vol. 61, no. 4, pp. 1704-1713, 2013.
- [25] C. Tienda, M. Arrebola, J. A. Encinar, and G. Toso, "Analysis of a dual-reflector antenna,"

- IET Microwave Antennas & Propagation*, vol. 5, no. 13, pp. 1636-1645, 2011.
- [26] W. Menzel, M. Al-Tikriti, and R. Leberer, "A 76 GHz multiple-beam planar reflector antenna," *European Microw. Conf.*, Milano, Italy, pp. 977-980, Sept. 2002.
- [27] H. M. Braun and P. E. Knobloch, "SAR on small satellites-shown on the SAR-Lupe example," *Proceedings of the International Radar Symposium*, Cologne, Germany, Sept. 5-7, 2007.
- [28] C. Wan and J. A. Encinar, "Efficient computation of generalized scattering matrix for analyzing multilayered periodic structures," *IEEE Trans. Antennas Propag.*, vol. 43, no. 10, pp. 233-1242, 1995.
- [29] C. Tienda, J. A. Encinar, M. Arrebola, M. Barba, and E. Carrasco, "Design, manufacturing and test of a dual-reflectarray antenna with improved bandwidth and reduced cross-polarization," *IEEE Trans. Antennas Propag.*, vol. 61, no. 3, pp. 1180-1190, 2012.
- [30] J. A. Encinar, L. She Datashvili, J. A. Zornoza, M. Arrebola, M. Sierra-Castaner, J. L. Besada-Sanmartin, H. Baier, and H. Legay, "Dual-polarization dual-coverage reflectarray for space applications," *IEEE Trans. Antennas Propag.*, vol. 54, no. 10, pp. 2827-2837, 2006.
- [31] J. A. Encinar, M. Arrebola, L. F. de la Fuente, and G. Toso, "A transmit-receive reflectarray antenna for direct broadcast satellite applications," *IEEE Trans. Antennas Propagation*, vol. 59, no. 9, pp. 3255-3264, 2011.
- [32] J. A. Encinar, M. Arrebola, M. Dejus, and C. Jouve, "Design of a 1-metre reflectarray for DBS application with 15% bandwidth," *First European Conference on Antennas and Propagation, Davos*, Switzerland, pp. 1-5, Nov. 6-10, 2006.
- [33] R. Leberer and W. Menzel, "A dual planar reflectarray with synthesized phase and amplitude distribution," *IEEE Trans. Antennas Propag.*, vol. 53, no. 11, 2005.
- [34] J. A. Zornoza, R. Leberer, J. A. Encinar, and W. Menzel, "Folded multi-layer microstrip reflectarray with shaped pattern," *IEEE Trans. Antennas Propag.*, vol. 54, pp. 510-518, 2006.
- [35] J. E. Hansen, "Spherical near-field antenna measurements," *IEE Electromagnetic Waves Series 26*.
- [36] M. Arrebola, Y. Alvarez, J. A. Encinar, and F. Las-Heras, "Accurate analysis of printed reflectarrays considering the near field of the primary feed," *IET Microw., Antennas Propag.*, vol. 3, no. 2, pp. 187-194, 2009.
- [37] K. Pontoppidan, Technical Description of GRASP8 (TICRA).
- [38] O. Bucci, "Intersection approach to array pattern

synthesis," *IEE Proceedings*, vol. 137, no. 6, pp. 349-57, 1990.



Carolina Tienda was born in Málaga and she currently resides in Munich, Germany. She received the Telecommunication Engineer degree from the Universidad de Málaga (UMA), Málaga, Spain, in October 2005, and the Telecommunication Ph.D. degree from the Universidad Politécnica de Madrid (UPM), Spain, in March 2012.

From October 2005 to April 2006, she was with the Communications Department, UMA as a Project Assistant. From April 2006 to April 2008, she was working as an RF & Antenna Engineer for INDRA ESPACIO, Madrid, Spain. In May 2008, she joined the Antenna and Sub-Millimeter Wave Section, Electromagnetic Division, European Space Agency ESTEC, The Netherlands, where she worked as Spanish Trainee. From May 2010 to June 2012, Tienda was with the Electromagnetism and Circuits Theory Department at Universidad Politécnica de Madrid (UPM), Spain, as Antenna Researcher. Tienda participated in different research projects supported by the Spanish Government and the European Space Agency (ESA). Since October 2012, she is with the Radar Concepts Department at the German Aerospace Center (DLR). Her current research interests include the analysis and design of space antennas, particularly Digital Beam Forming parabolic reflector antennas and printed reflectarray antennas in single and dual reflectarray configurations.



José A. Encinar (S'81-M'86-SM'09-FM'10) was born in Madrid, Spain. He received the Electrical Engineer and Ph.D. degrees, both from Universidad Politécnica de Madrid (UPM), in 1979 and 1985, respectively. Since January 1980 has been with the Applied Electromagnetism and Microwaves Group at UPM, as a Teaching and Research Assistant from 1980 to 1982, as an Assistant Professor from 1983 to 1986, and as Associate Professor from 1986 to 1991. From February to October of 1987 he stayed at Polytechnic University, Brooklyn, NY, as a Post-doctoral Fellow of the NATO Science Program. Since 1991 he is a Professor of the Electromagnetism and Circuit Theory Department at UPM. He was with the Laboratory of Electromagnetics and Acoustics at Ecole Polytechnique Fédérale de

Lausanne (EPFL), Switzerland in 1996, and with the Institute of Electronics, Communication and Information Technology (ECIT), Queen's University Belfast, U.K. in 2006 and 2011, as a Visiting Professor. His research interests include numerical techniques for the analysis of multi-layer periodic structures, design of frequency selective surfaces, printed arrays and reflectarrays. Encinar has published more than one hundred and fifty journal and conference papers, and he is holder of five patents on array and reflectarray antennas. He was a co-recipient of the 2005 H. A. Wheeler Applications Prize Paper Award and the 2007 S. A. Schelkunoff Transactions Prize Paper Award, given by IEEE Antennas and Propagation Society. He has been a Member of the Technical Programme Comity of several International Conferences (European Conference on Antennas and Propagation, ESA Antenna Workshops, Loughborough Antennas & Propagation Conference). He is an IEEE Fellow Member.



Mariano Barba was born in Murcia, Spain. He received the Ingeniero de Telecomunicación and Ph.D. degrees from the Universidad Politécnica de Madrid, Madrid (UPM), Spain, in 1990 and 1996, respectively. From 1991 to 1994 he was with the Depto. de Electromagnetismo y Teoría de Circuitos (UPM) as postgraduate researcher. During this time, he developed numerical methods and algorithms to characterize and design microwave passive devices. From 1994 to 2002, he has been involved in the R&D departments of several companies and institutions developing antennas and microwave circuits for space and terrestrial

communication applications. In 2002, he joined to the "Depto. de Electromagnetismo y Teoría de Circuitos", (UPM) as Associate Professor. His research interests include the analysis, characterization and design of antenna and microwave circuits. He is currently involved in the development and design of multibeam and reconfigurable antennas.



Manuel Arrebola (S'99-M'07) was born in Lucena (Córdoba), Spain. He received the Ingeniero de Telecomunicación degree from the Universidad de Málaga (UMA), Málaga, Spain, in 2002, and the Ph.D. degree from the Universidad Politécnica de Madrid (UPM), Madrid, Spain, in 2008. From 2003 to 2007 he was with the Electromagnetism and Circuit Theory Department at UPM as a Research Assistant. From August to December 2005, he was with the Microwave Techniques Department at the Universität Ulm, Ulm, Germany, as a Visiting Scholar. In December 2007, he joined the Electrical Engineering Department at the Universidad de Oviedo, Gijón, Spain, where he is an Associate Professor. In 2009, he enjoyed a two-month stay at the European Space Research and Technology Centre, European Space Agency (ESTE-ESA), Noordwijk, The Netherlands. His current research interests include analysis and design techniques of contoured-beam and reconfigurable printed reflectarrays both in single and dual-reflector configurations and planar antennas. Arrebola was co-recipient of the 2007 S. A. Schelkunoff Transactions Prize Paper Award, given by IEEE Antennas and Propagation Society.